Available online at www.worldnewsnaturalsciences.com

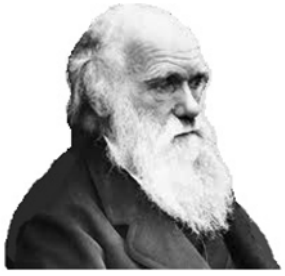

World News of Natural Sciences

WNOFNS 15 (2017) 1-19 EISSN 2543-5426

Experimental study on the inhibitive effect of phytic acid as a corrosion inhibitor for Q235 mild steel in 1 M HCl environment

Maduabuchi A. Chidiebere

Electrochemistry and Materials Science Research Laboratory, Department of Chemistry, Federal University of Technology, Owerri, PMB 1526, Owerri, Nigeria
E-mail address: arinzechukwuchidiebere@gmail.com

Simeon, Nwanonenyi

Electrochemistry and Materials Science Research Laboratory, Department of Chemistry, Federal University of Technology, Owerri, PMB 1526, Owerri, Nigeria
E-mail address: demianifeanyi@gmail.com

Demian Njoku

Institute of Metal Research, Chinese Academy of Sciences, 62 Wencui Rd, Shenyang, 110016, China
E-mail address: simyn22@yahoo.co.uk

Nkem B. Iroha

Department of Chemistry, Federal University Otuoke, Yenagoa, Nigeria
E-mail address: nkemib@yahoo.com

Emeka E. Oguzie

Electrochemistry and Materials Science Research Laboratory, Department of Chemistry, Federal University of Technology, Owerri, PMB 1526, Owerri, Nigeria
E-mail address: emekaoguzie@gmail.com

Ying Li

Institute of Metal Research, Chinese Academy of Sciences, 62 Wencui Rd, Shenyang, 110016, China
E-mail address: liying@imr.ac.cn

ABSTRACT

The inhibitive action of phytic acid (PA) on Q235 mild steel corrosion in 1 M HCl environment was investigated using electrochemical techniques. Polarization results revealed PA to be a mixed-type inhibitor in 1 M HCl environment, while impedance results provide evidence of adsorption of the PA species on the corroding metal surface. The adsorption of PA obeyed Langmuir adsorption isotherm. Scanning electron microscopy (SEM), atomic force microscopy (AFM) and Fourier transform infrared spectroscopy (FTIR) studies all revealed the formation of a protective film adsorbed on the steel surface.

***Keywords*:** Adsorption, Corrosion, Electrochemical techniques, Inhibition, Metals, Plant extract

1. INTRODUCTION

In order to lessen mild steel corrosion, one of the most effective solution is to set apart the metal from aggresive species using corrosion inhibitors. Most inorganic substances (phosphates, chromates, dichromate and arsenates) have been proven to be good inhibitors of metal corrosion, but a major disadvantage is that they are really unsafe to health and the environment as well, and have come under increasing ecological scrutiny and stringent environmental regulations. Current research efforts now centres on the development of safe, cheap and corrosion inhibitors that are safe as alternatives.

Chemical compounds, having Nitrogen, oxygen, sulphur etc in a conjugated system are good inhibitors which impedes the corrosion of metals in harsh solutions [Pourbaix M, 1974; Nisancioglu K, 1992; Gomma G K, 1998; Umoren *et al*, 2006; Chidiebere *et al*, 2014; Ebenso E E, 2001; Oguzie *et al*, 2005; Oguzie *et al*, 2014; Umoren *et al*, 2010; Oguzie *et al*, 2009]. They operate by adsorbing onto the mild steel surface, and thus form protective layers that slows down the corrosion reaction. Considering the adsorption ability of inhibitors, some factors must be considered they include: the type and charge present on the metal under study, species present in the electrolyte and also, the structure of the compound used as inhibitor.

It is obvious that phytic acid is useful in this regard. Phytic acid (PA) is safe and soluble in water. It serves as a depigmenting substitute espeially in cosmetic emulsions [André & Jivaldo, 2013]. PA has a molecular mass and formular of 660g/mol and $C_6H_{18}O_{24}P_6$. The structure is shown in Figure 1. From the constituents (oxygen and phosphorus) of the structure of PA and the molecular weight one can decide that it should be a good corrosion inhibitor. Phytic acid has been shown to be effective as corrosion inhibitor [Hongyun *et al*, 2011; Sheng *et al*, 2009] However, further studies are required to understand the inhibition mechanism, in hydrchloric acid environment.

The purpose of this study is to advance the use of safe inhibitors for protection of metals and also, reports on the inhibiting strength of PA on Q235 mild steel corrosion in 1 M HCl environment. Careful perusal of PA structure in Figure 1 shows the presence of some heteroatoms like oxygen and also, aromatic ring which plays a useful role in corrosion inhibition of metals. The inhibiting efficacy was determined using electrochemical methods. The mild steel surface in the uninhibited and inhibited solution has been pictured by SEM and AFM. Theoretical calculations were adopted to correlate the inhibition ability of PA with its electronic structural parameters [Khaled K. F, 2010; Oguzie *et al*, 2010**;** Umoren & Ebenso, 2007; Solmaz *et al*, 2008]

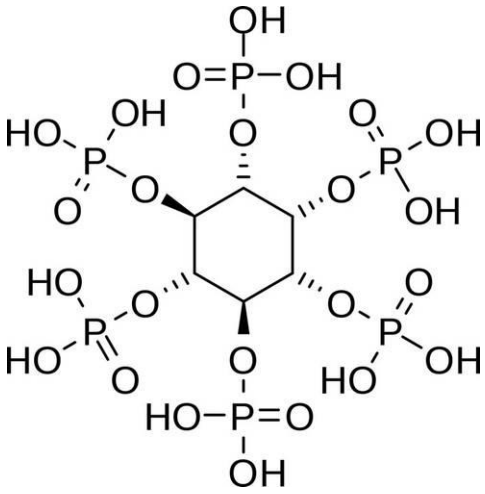

Figure 1. Structure of phytic acid.

2. MATERIALS AND METHODS

2. 1. MATERIALS

Q235 mild steel couponss of the composition (weight %) C -0.30, Si – 0.30, Mn – 0.30, P – 0.045, S – 0.050, Cr – 0.064, Cu – 0.040, Ti – 0.04 and the balance Fe were used for the studies. They coupons were polished using silicon carbide abrasive paper (from grade #240 – #1000), the metal coupons were degreased using acetone, thereafter it was cleaned using distilled water and dried in warm air. Chemicals used for preparation of the test solutions were of analytical grade (Sinopharm Chemical Reagent Co., Ltd). Distilled water was used in the solution preparations. Experiments were carried out using different concentrations of PA (0.0005 M, 0.001 M, 0.002 M and 0.005 M), respectively. Experiments were performed at 30±1 °C and non-deaerated solutions.

2. 2. ELECTROCHEMICAL METHODS

This aspect of the experiment was carried out in a standard three-electrode glass cell of 500 ml capacity using an Advanced Electrochemical System workstation (PARC Parstart-2273). A platinum foil served as counter electrode and, a saturated calomel electrode (SCE) was used as reference electrodes. A mild steel specimen of 1 cm^2 dimension was used as working electrode. Electrochemical measurements were carried out at 30±1 °C, using standard procedures, in aerated solutions at the end of 1800s of immersion, which allowed the OCP values to attain steady state. Measurements were carried out at the corrosion potentials (E_{corr}) over a frequency range of 100 kHz – 10 mHz, with a signal amplitude of 5 mV. Impedance data was analyzed using Zsimpwin 3.0 software.

The Potentiodynamic polarization (PDP) experiments were conducted at a scan rate of 0.333 mV/s. The potential range employed was ±250 mV versus corrosion potential. For analyzing the polarization data, Powersuite software was used [Chidiebere *et al*, 2012].

2. 3. SCANNING ELECTRON MICROSCOPY

The XL-30FEG scanning electron microscope was employed to picture the surface of the metal coupons after immersion in the test soluton. This was done in the absence and presence of PA. Mild steel coupons of dimensions 3 cm × 3 cm × 0.25 cm were prepared as shown in Section 2.1 and immersed for 24 h in the test solutions, in the absence and presence of 0.001 M PA. The coupons were taken out and washed with distilled water, dried in cool air and used for SEM scrutiny. Also, EDX study was carried out for mld steel dipped in the inhibited and uninhibited solutions to determine the elemental contents of the adsorbed layer.

2. 4. ATOMIC FORCE MICROSCOPY

AFM observation was carried out with the aid of Picoplus 2500 surface probe microscope. Mild steel specimens with dimensions 15×15×2 mm were dipped in the different test solutions for 24 h in the absence and presence of 0.001 M PA at 30 ± 1 °C. After removal, the specimens were cleaned with double distilled water, dried in warm air and submitted for AFM observation.

2. 5. FTIR SPECTROSCOPY

Fourier transform infrared (FTIR) spectra (KBr) were recorded using a Nicolet Magna-IR 560 FTIR spectrophotometer. The spectra for PA as well as the film layer formed/adsorbed on the mild steel surface after 24 h immersion in 1 M HCl solution containing 0.001 M PA were recorded by scrapping the film, mixing it with KBr, and making the pellets.

3. RESULTS AND DISCUSSION

3. 1. ELECTROCHEMICAL METHODS

Corrosion reaction involves an electrochemical process and therefore, electrochemical measurements are reliable to throw comprehensive understanding of the corrosion process. Studies were carried out to observe the influence of various concentrations of PA on the electrochemical corrosion behavior of mild steel in the test solution.

3. 1. 1. POTENTIODYNAMIC POLARIZATION MEASUREMENTS

Polarization tests were done to assess the efficacy of PA in impeding the electrochemical partial reactions [Umoren *et al*, 2013]. In Figure 2, what we have there is a picture of polarization curves for the mild steel specimens in the investigated environment, in the absence and presence of PA. The mild steel specimen revealed active dissolution and there was no proof of passivation in the studied potential range. The corresponding electrochemical parameters, namely, corrosion potential (E_{corr}), corrosion current density (I_{corr}), anodic (b_a) and cathodic (b_c) Tafel slopes were obtained and their values are shown in Table 1. The data shown therein reveals that when PA was added the I_{corr} decreased compared to the uninhibited solution and this tendency continued with an increase in the concentration of PA, nevertheless, at higher concentration, the corrosion current density (I_{corr}) increased a little from 0.002 M PA to 0.005 M PA. Hence there is increase in concentration, there is the probability of having some free PA molecules in the acid solution. For this reason, the observed increase in corrosion current could be as a result of counteraction between the free

PA molecules to form a protective film on the metal surface. As expected, the addition of the inhibitor impeded the anodic metal dissolution process and also the cathodic H^+ ion reduction [Negam *et al*, 2011; Sappani & Sambantham, 2013], but no outstanding effect was noticed on the E_{corr} values. It has been suggested that if the displacement in E_{corr} on addition of inhibitor exceeds 85 mV, the inhibitor could be classified as cathodic or anodic type and if the displacement is lower than 85 mV, then the inhibitor may be regarded as mixed-type [Wang *et al*, 2011]. What was observed in this study revealed that PA behaved as a mixed type inhibitor. Also, at over voltages that are higher than circa -350 mV (SCE), it was noticed that metal dissolution was more compared to PA adsorption.

The values of the corrosion current density in the absence and presence of the inhibitor were used to calculate the inhibition efficiency from polarization data as follows:

$$IE\% = \left(\frac{I_{corr(bl)} - I_{corr(inh)}}{I_{corr(bl)}}\right) x\ 100 \qquad (1)$$

The obtained values presented in Table 1 reveal that IE increased with PA concentration, however, a decreased was observed at higher concentrations.

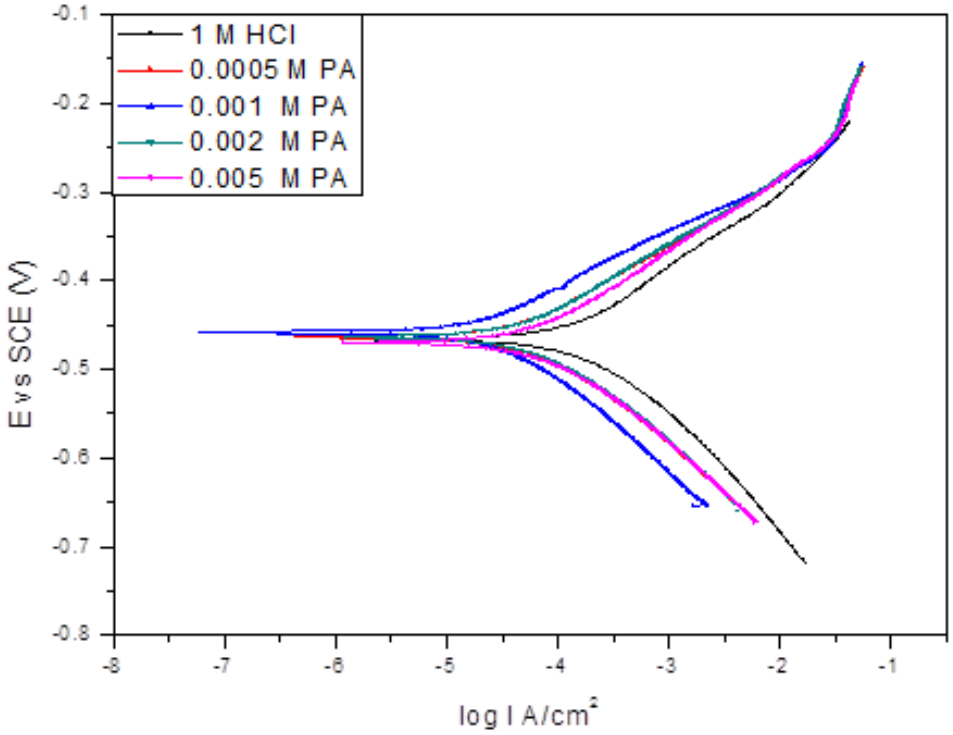

Figure 2. Potentiodynamic polarization curves of mild steel in 1 M HCl solution in the absence and presence of PA.

Table 1. Polarization parameters for mild steel in 1 M HCl in the absence and presence of PA

System	E_{corr} (mV vs SCE)	I_{corr} (μA cm^{-2})	ba (mV dec^{-1})	bc (mV dec^{-1})	IE (%)
1 M HCl	-466.4	183	122.7	100.5	
0.0005 M PA	-463.7	71.8	96.8	107.5	60.7
0.001 M PA	-458.3	34.8	87.5	108.2	80.9
0.002 M PA	-463.2	76.3	98.7	107.9	58.3
0.005 M PA	-469.6	85.3	98.7	107.8	53.4

3. 1. 2. ELECTROCHEMICAL IMPEDANCE SPECTROSCOPY MEASUREMENTS

Figure 3a-c denote the Nyquist, Bode phase angle and Bode modulus graphs for mild steel in 1 M HCl in the absence and presence of various concentrations of PA. The Nyquist plots show one semicircles over the frequency range studied, this relates to one time constant in the Bode plots. The areas of high frequency intercept with their real axis in the Nyquist plots are attributed to the solution resistance (R_s) and the areas of low frequency intercept with their real axis are related to the charge transfer resistance (R_{ct}). It was obvious, as shown in Figure 3, that when PA was added in the test solution an increase in the magnitude of the bode plots was observed, these measurements suggests inhibition of the corrosion measure.

The measured values of the various impedance parameters shown in Table 2, were extrapolated by fitting to the relevant circuit models $R_s(Q_{dl}R_{ct})$, which have been employed earlier to model the metal/acid interface [Obot & Obi-Egbedi, 2010; Tao *et al*, 2011; Kissi *et al*, 2006]. Here we used CPE in place of a capacitor just to take care of deviations from ideal dielectric behavior resulting from the inhomogeneous nature of the electrode surfaces. The impedance of the CPE is given by;

$$Z_{CPE} = Q^{-1}(j\omega)^{-n} \qquad (2)$$

where Q and n stand for the CPE constant and exponent, respectively, $j^2 = -1$ is an imaginary number, and ω is the angular frequency in rad s^{-1} ($\omega = 2\pi f$ when f is the frequency in Hz), CPE can represent resistance ($Z_{CPE} = R$, $n = 0$), capacitance ($Z_{CPE} = C$, $n = 1$). Considering the data presented in Table 2, it is clear that PA increased the R_{ct} values at all concentrations compared with the uninhibited solution.

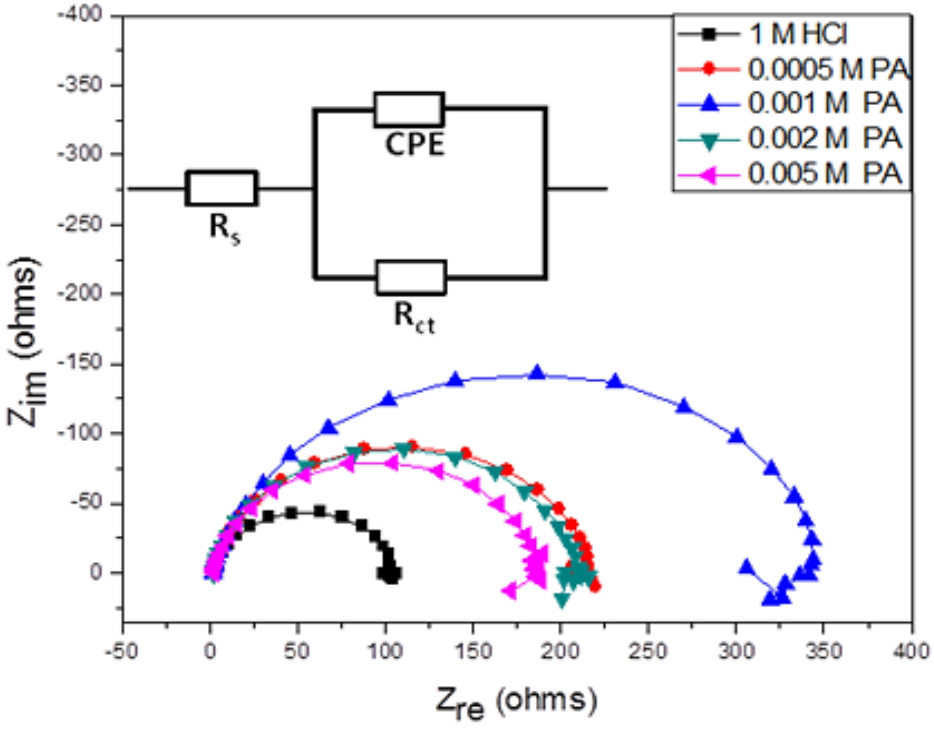
1 M HCl
0.0005 M PA
0.001 M PA
0.002 M PA
0.005 M PA
CPE
R_s
R_{ct}
Z_{im} (ohms)
Z_{re} (ohms)

(a)

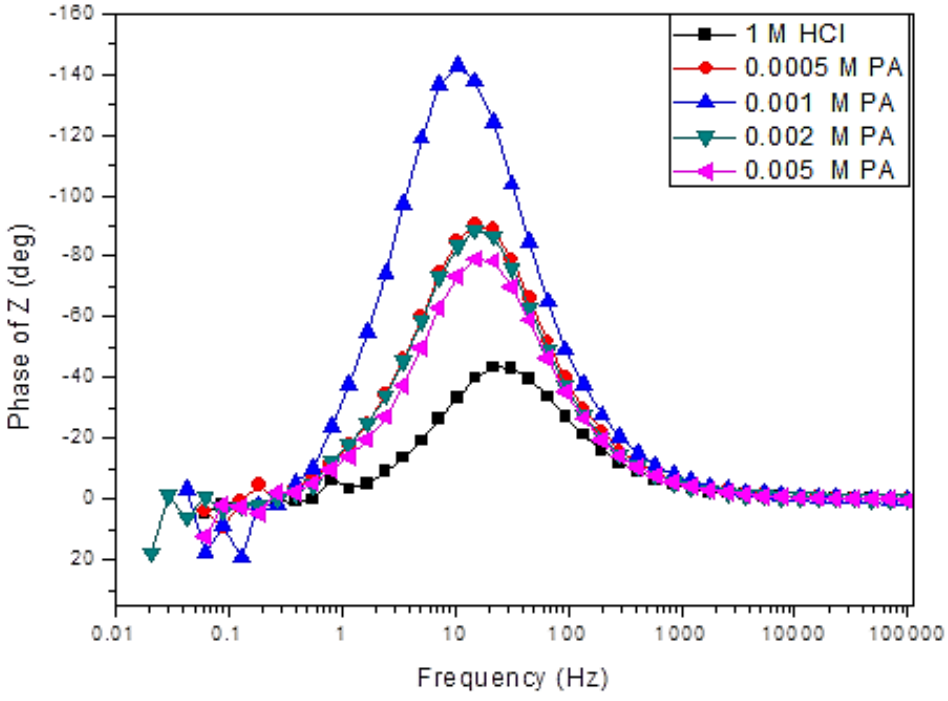
1 M HCl
0.0005 M PA
0.001 M PA
0.002 M PA
0.005 M PA
Phase of Z (deg)
Frequency (Hz)

(b)

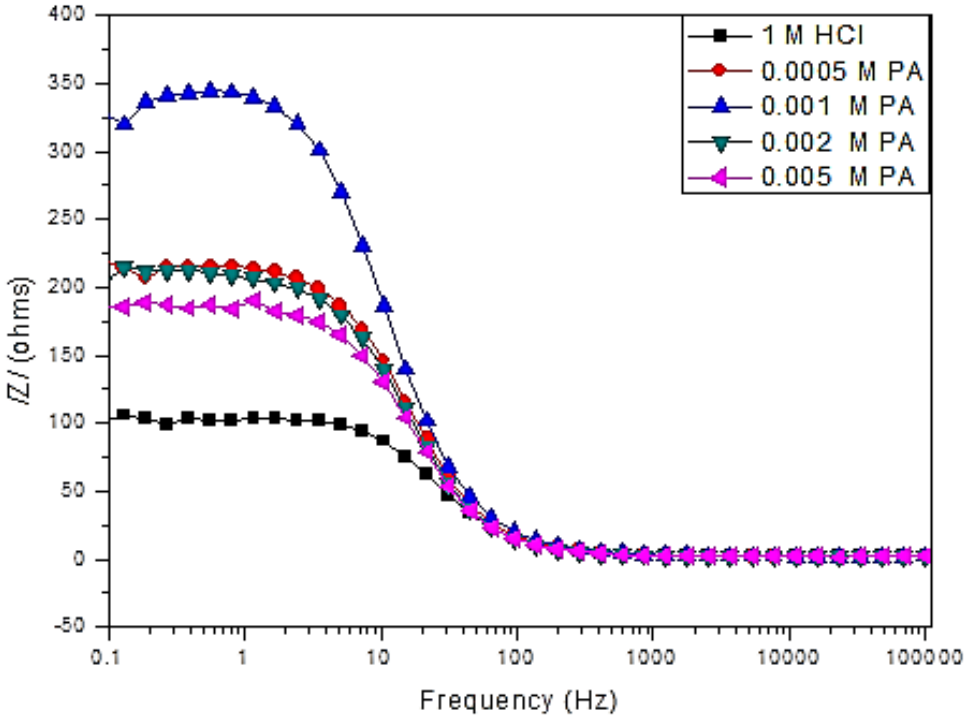

(c)

Figure 3. Electrochemical impedance spectra of mild steel in 1 M HCl solution in the absence and presence of PA: (a) Nyquist, (b) Bode phase angle and (c) Bode modulus plots.

Modification of the interface by adsorbed inhibitor lowered the values of C_{dl}, according to Helmholtz model [Chidiebere *et al*, 2012]:

$$C_{dl} = \frac{\varepsilon \varepsilon_o A}{\delta} \qquad (3)$$

ε simply represents the dielectric constant of the medium, ε_o is the vacuum permittivity, A is the electrode area, and δ is the thickness of the interfacial layer. The observed decrease in Q_{dl} value thus results from a decrease in the dielectric constant and/or an increase in the double layer thickness, due to the adsorption of PA on the corroding steel surface. This involves the replacement of water molecules by the inhibitor species which has smaller dielectric constants. The increase in resistance with PA concentration, suggests increased adsorption of PA molecules on the metal surface, leading to the protection of the steel surface [Prabhu *et al*, 2008; Moretti *et al*, 2003].

The inhibition efficiency (*IE %*) from impedance data was calculated by comparing the values of the charge transfer resistance in the absence and presence of PA as follows:

$$IE\% = \left(\frac{R_{ct(inh)} - R_{ct}}{R_{ct(inh)}} \right) x\ 100 \qquad (4)$$

Where R_{ct} and $R_{ct\ (Inh)}$ denotes charge transfer resistance in the absence and presence of the inhibitor. The obtained IE values are presented in Table 2. The data corresponds with the polarization results.

Table 2. Electrochemical impedance parameters of mild steel in 1 M HCl in the absence and presence of PA.

System	R_s (Ω cm^2)	R_{ct} (Ω cm^2)	N	C_{dl} ($\mu\Omega^{-1}S^n cm^{-2}$)	IE (%)
1 M HCl	1.738	102.6	0.89	2.340E-5	
0.0005 M PA	1.826	214.5	0.89	1.050E-5	51.2
0.001 M PA	1.854	338.5	0.88	6.595E-6	69.7
0.002 M PA	1.796	207.2	0.91	1.069E-5	50.5
0.005 M PA	1.782	185.5	0.90	1.210E-5	44.7

3. 1. 3. EFFECT OF IMMERSION TIME

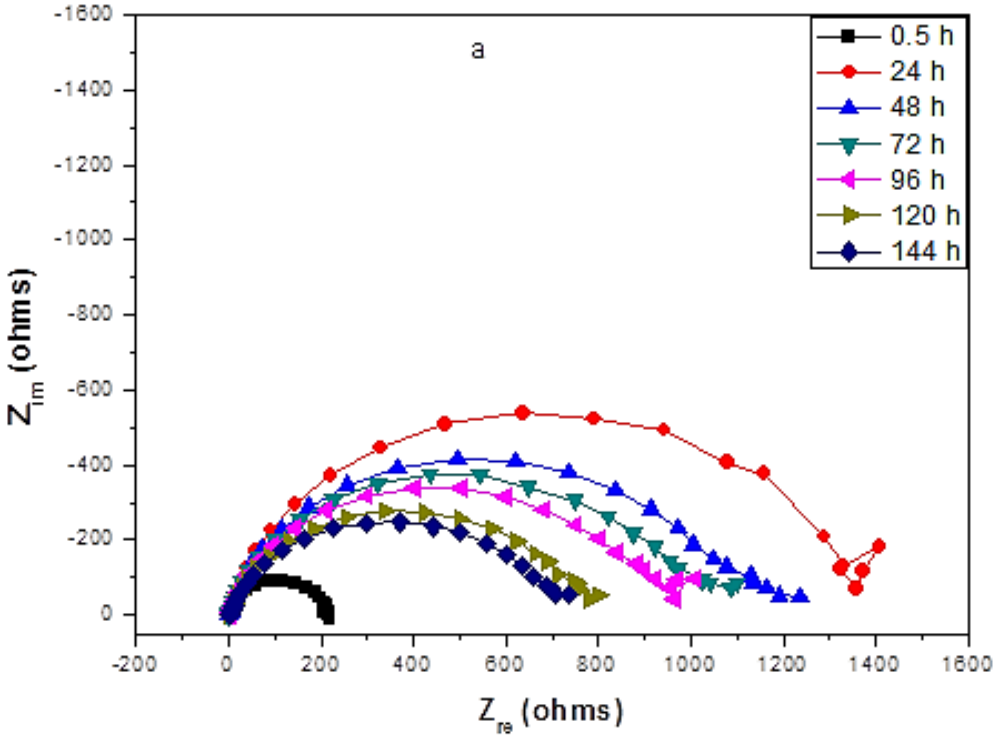

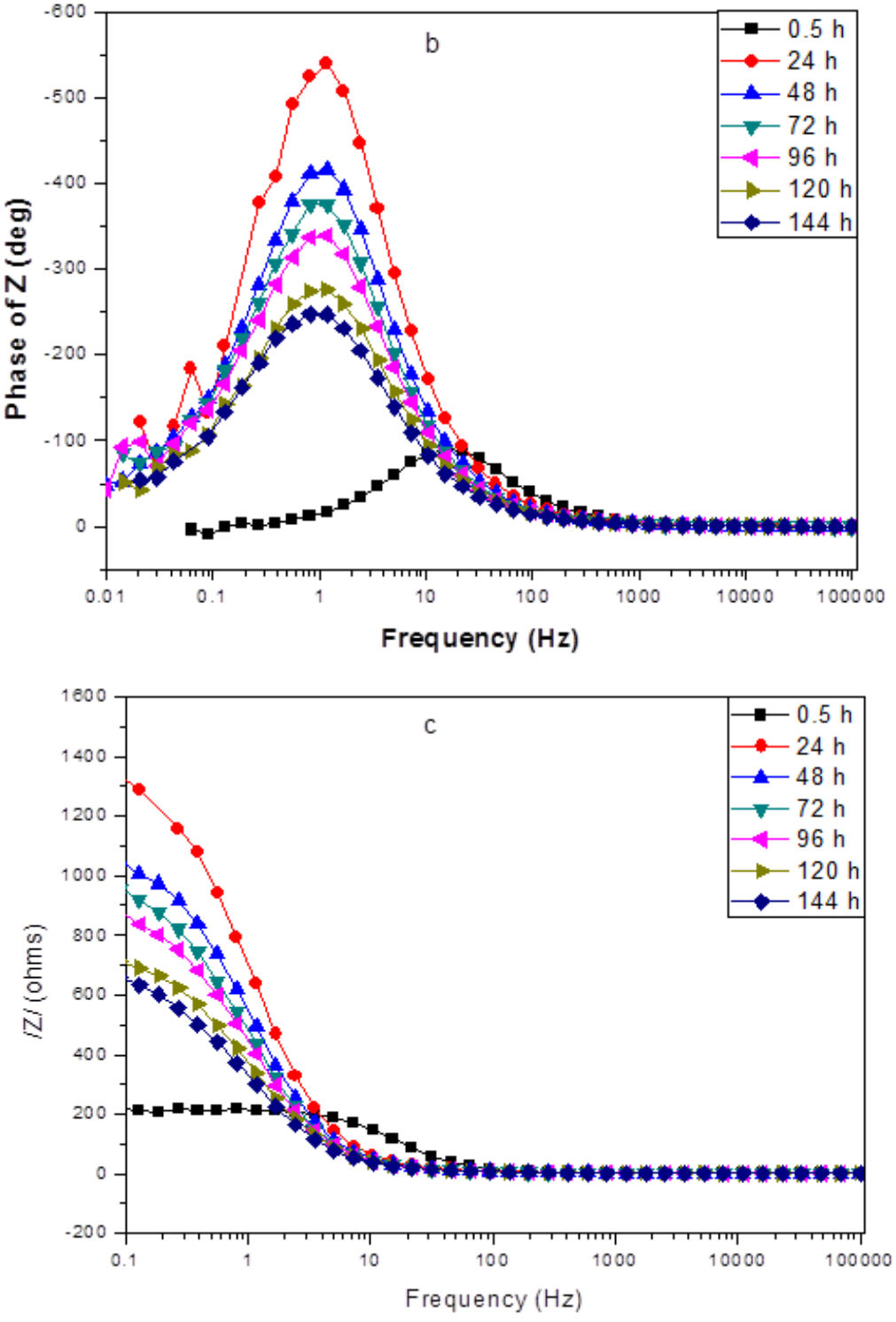

Figure 4. Electrochemical impedance spectra of mild steel in 1 M HCl in the absence and presence of 0.0005 M PA: (a) Nyquist (b) Bode phase angle and (c) Bode modulus plots.

Figure 4 shows the electrochemical impedance plot obtained over a period of 144 h in the presence of 0.0005 M PA. Close observation of the impedance spectra, show that immersion time has a noticeable effect on the corrosion strenght of PA. The obtained data are presented in Table 3. It is apparent from the Nyquist (4a), Bode phase angle (4b), and Bode modulus (4c) plots that corrosion resistance increased considerably, going from 0.5 h (R_{ct} = 214.5 Ω cm^2) to 24 h of immersion (R_{ct} = 1392 Ω cm^2), decreased steadily thereafter.

As expected, the corresponding Q_{dl} values suggests that processes existing between the metal/test solution interface at the begining increased the thickness (or compact) of the inhibitor layer within the initial 24 h, while increasing Q_{dl} values with more increase in immesion time suggest reduced compactness of the adsorbed inhibitor layer, which permits increased ingress of the corrosive species, hence reduced corrosion resistance. The same reason is applicable to the trend observed in the case of Rct values.

Table 3. Effect of immersion time on the impedance response of mild steel in 1 M HCl containing 0.0005 M PA.

System	R_s (Ω cm^2)	R_{ct} (Ω cm^2)	n	C_{dl} (μΩ$^{-1}S^n cm^{-2}$)
0.5 h 0.0005 M PA	1.826	214.5	0.89	1.050E-5
24 h 0.0005 M PA	1.675	1392	0.84	1.580E-6
48 h 0.0005 M PA	1.669	1139	0.83	1.940E-6
72 h 0.0005 M PA	1.649	1037	0.83	2.181E-6
96 h 0.0005 M PA	1.595	955.5	0.81	2.409E-6
120 h 0.0005 M PA	1.609	778.6	0.80	3.028E-6
144 h 0.0005 M PA	1.573	722.6	0.78	3.347E-6

3. 2. SCANNING ELECTRON MICROSCOPY

Clear picture of the surface morphologies of the mild steel immersed in the test acid environment in absence and presence of PA are presented in Figure 5. The images show that the surface of mild steel in the absence of the inhibitor is not smooth due to active dissolution of the metal. However, the roughness reduced significantly on addition of PA to the acidic environment. The result reveals that the introduction of PA molecules reduced the active dissolution of mild steel by formation of a protective layer on its surface.

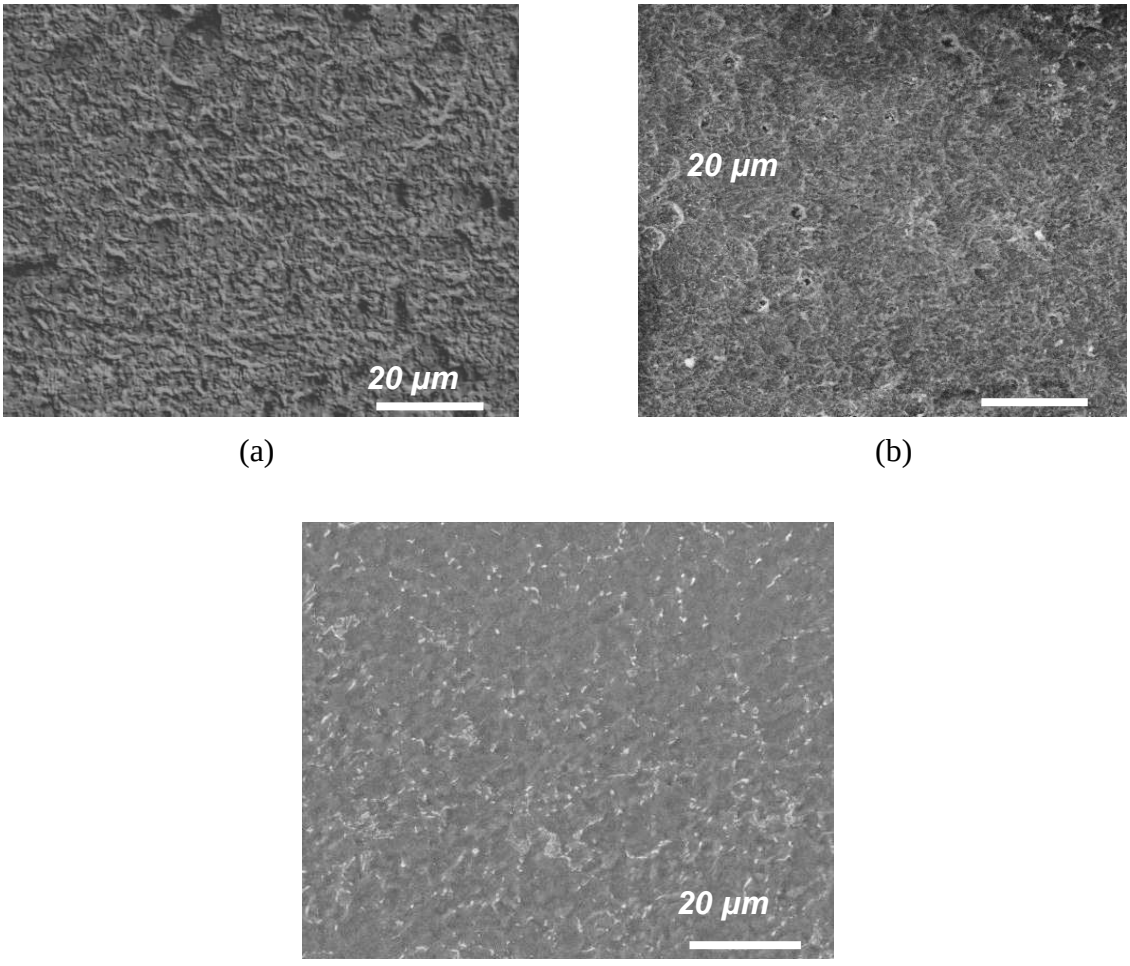

(a) (b)

(c)

Figure 5. SEM images of the mild steel surface after 24 h immersion at 30 °C in 1 M HCl solution in the; (a) absence of PA (b) presence of 0.0005 M PA, and (c) presence of 0.001 M PA, respectively.

Close scrutiny of the images in Figure 5b and c reveal that the mild steel surface was more protected in 0.001 M PA (Fig. 5c) compared to 0.0005 M PA (Fig. 5b). This suggests the presence of a more compact/stronger protective layer formed on metal surface at this concentration; in agreement with the higher inhibition efficiency obtained therein.

3. 2. 1. EDX ANALYSIS

This technique was employed to determine the presence of some elements on the metal surface before and after it was dipped into the inhibitor solution. The result presented in Figure 6 shows clearly the EDX spectra for the corrosion materials formed on mild steel surface in the uninhibited and inhibited solution. In the uninhibited solution, the spectrum confirms the presence of Fe and oxygen, this is as a result of the formation of oxides and

some mild steel composites. Also, the presence of carbon and phosphorus was not observed, however, in the presence of the optimum concentration of the PA, phosphorus and carbon atoms are found to be present on the mild steel surface (Fig 6b). This reveals that the phosphorus and carbon atoms contained in the inhibitor molecules actually adsorbed on the metal surface, hence its ability to protect the mild steel surface against corrosion.

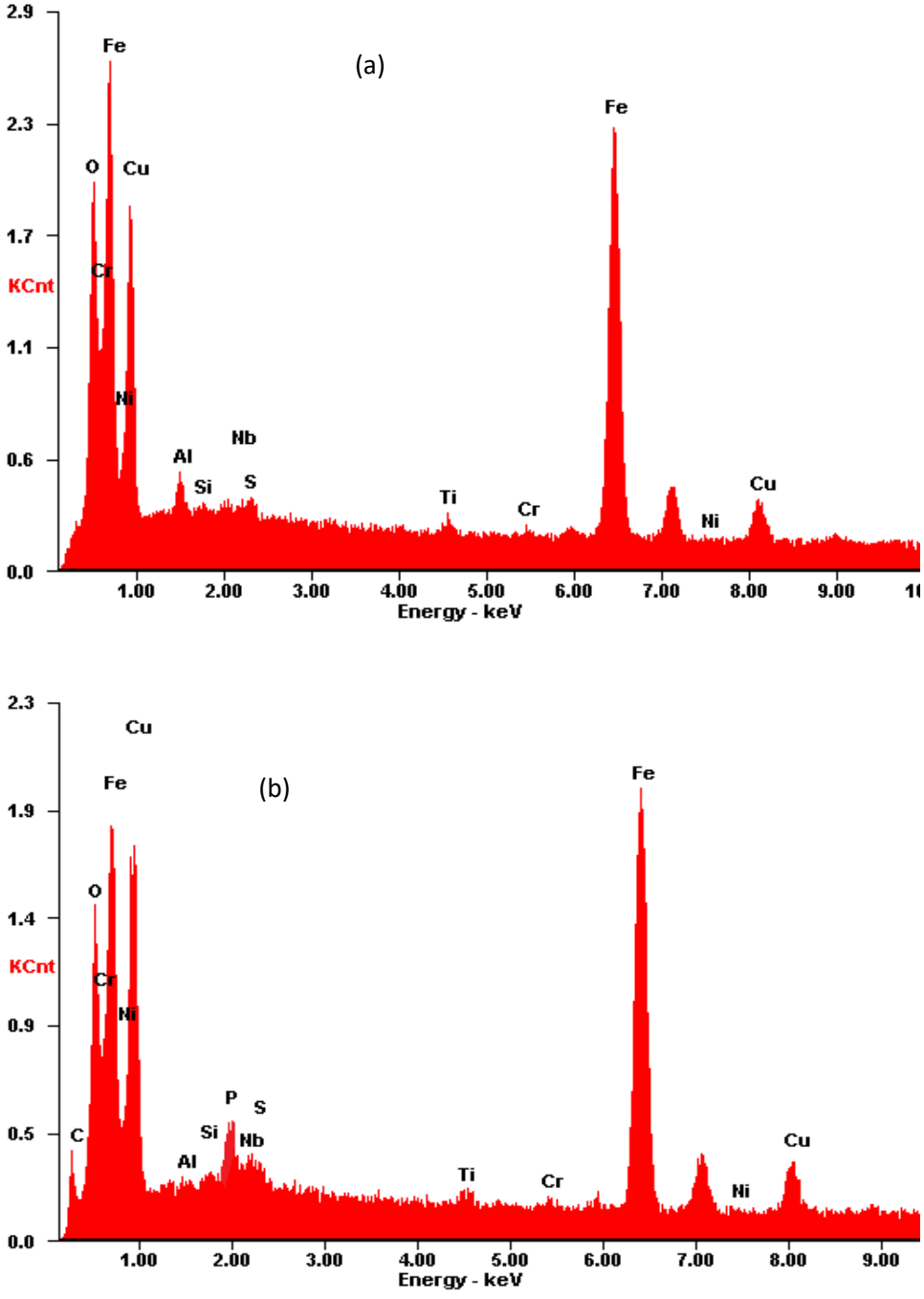

Figure 6. EDX spectra of mild steel surface immersed for 24 h in: (a) 1 M HCl and b) 0.001 M PA.

3. 3. ATOMIC FORCE MICROSCOPY

AFM analysis was performed to investigate the surface morphology and also, the influence of PA on the progress of corrosion on the metal surface. Figures 7a and b depict the three dimensional (3D) AFM morphologies of mild steel in 1 M HCl in the absence and presence of 0.001 M PA and 0.0005 M PA. Close scrutiny of the image in Figure 7a reveals that the surface is rough due to aggressive corrosion attack in the absence of the inhibitor.

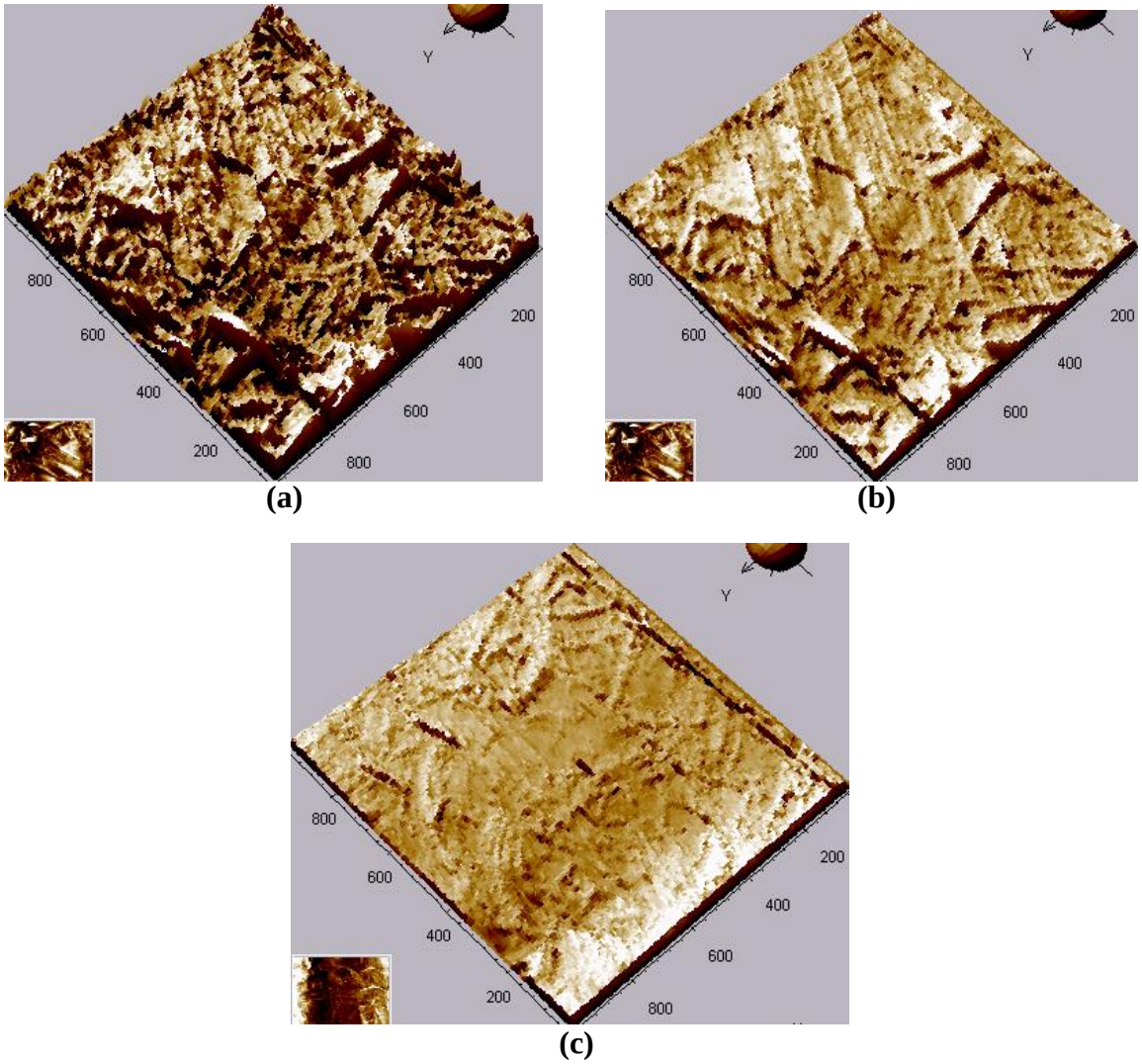

Figure 7. The three dimensional (3D) AFM morphologies for mild steel in: (a) absence, (b) presence of 0.0005 M PA and (c) presence of 0.001 M PA, respectively.

In the presence of the inhibitor (Figure 7b and c) a new/smooth surface morphology was observed, however, this was well noticeable at a higher concentration of 0.001 M PA. One can correlate this to the adsorbed PA molecules onto the metal surface. The obtained result is in good agreement with the electrochemical and SEM results.

3. 4. FTIR ANALYSIS

FT-IR spectrum of the PA sample presented in Figure 8, reveals the existence of some peaks attributed to functional groups. The spectra presented therein was used to make some comparism. As revealed, almost all the peaks in PA sample also were found in the surface film formed on the metal surface. This observation suggests that the functional groups in PA sample are as well present in the adsorbed thin layer. Close scrutiny of the peaks shows that some of the peaks deviated, while some vanished. The adsorption due to P-O and P=O stretching takes place at 770 cm^{-1} and 1190 cm^{-1}, C = O stretching frequency of PA has moved slightly from 1617 cm^{-1} to 1654 cm^{-1}, O-H stretching frequency from 3402 cm^{-1} to 3435 cm^{-1} , C=O and C-O stretching frequency from 1734 cm^{-1} to 1720 cm^{-1} and from 1240 cm^{-1} to 1098cm^{-1} [Kissi et al, 2006; Cornell, 1996; Mizushima et al, 1956; Jasinski & Lob, 1988], this shows the adsorption of PA on a corroding mild steel surface.

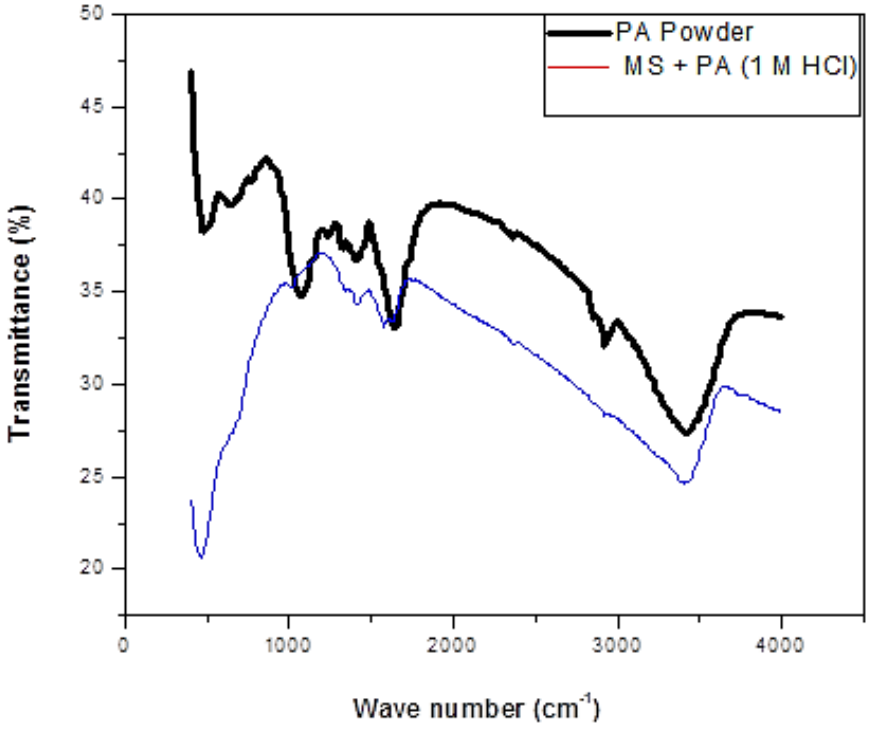

Figure 8. FTIR spectrum of phytic acid sample and the surface film on mild steel specimen immersed in 1 M HCl solution containing 0.001 M PA.

3. 5. ADSORPTION ISOTHERMS

The adsorption of PA on the metal surface is important and can be further understood from the adsorption isotherms [Asan *et al*, 2005]. According to the Langmuir adsorption isotherm;

$$\frac{C_{(inh)}}{\theta} = \frac{1}{K_{ads}} + C_{(inh)} \quad (5)$$

where $C_{(inh)}$ shows the inhibitor concentration, θ is the degree of surface coverage on the metal surface calculated from the equation θ = IE/100, as evaluated from polarization measurements [Kardas & Solmaz, 2006] and K_{ads} is the equilibrium constant for the adsorption/desorption process.

Figure 9 shows the plot of C/θ against C to be linear 1 M HCl environment, with slope of 1.29, suggesting that adsorption of PA molecules onto a metal surface obeys Langmuir adsorption isotherm. The obtained slopes of the straight plots deviated from unity; this can be correlated to the interactions between adsorbate species on the metal surface as well as changes in the adsorption heat with increasing surface coverage [Chidiebere, *et al*, 2012]. The obtained value for K_{ads} is 2327.1

The high value of K_{ads} shows strong adsorption ability of PA molecules on the metal surface [Solmaz *et al,* 2008] due to the presence of chloride ions, which is able to form intermediate bridges between the positively charged metal surface and protonated PA species.

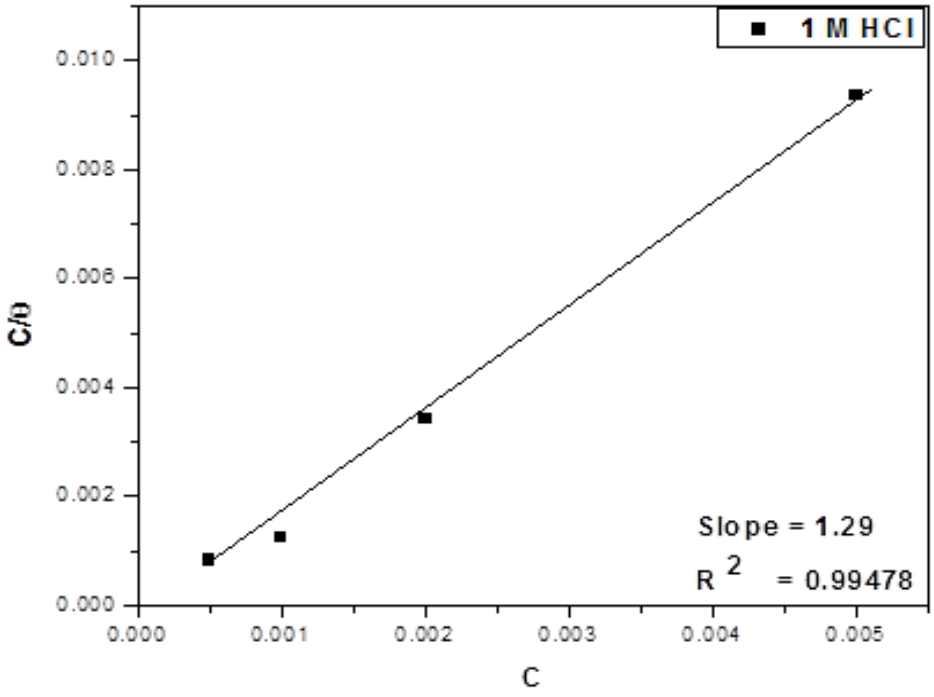

Figure 9. Langmuir adsorption isotherm plots for PA in 1 M HCl solution.

The adsorption/desorption equilibrium constant is connected to the standard free energy of adsorption (ΔG^{o}_{ads}) according to the equation: ΔG^{o}_{ads} = –RTIn (55.5K_{ads}), where R represents the universal gas constant and T is the absolute temperature. The obtained ΔG^{o}_{ads} value for PA is - 30 kJ mol^{-1}, this value exists between the values of - 20 kJ mol^{-1} and - 40 kJ mol^{-1} presumed for both physical and chemical adsorption [Negm *et al*, 2010; Obi-Egbedi & Obot, 2011; Özcan *et al*, 2008; Wang *et al*, 2011; Özcan *et al,* 2008; Deng *et al*, 2011].

4. CONCLUSIONS

(1) The investigation showed that PA is a potent inhibitor for mild steel corrosion in 1 M HCl solution.

(2) The inhibitor is a mixed-type one based on polarization studies, while evidence of adsorption of PA species on the metal surface was provided by the impedance data.

(3) Adsorption of PA obeys the Langmuir adsorption isotherm. The value of ΔG^{o}_{ads} corroborates firm and spontaneous correlation between PA and the mild steel surface.

(4) the surface morphological investigation revealed the existence of a protective layer adsorbed on a mild steel surface.

Acknowledgment

M. A. Chidiebere is grateful to the Chinese Academy of Sciences (CAS) and the Academy of Sciences for the Developing World (TWAS) for the award of CAS-TWAS Postgraduate Fellowship.

References

[1] M. Pourbaix, Atlas of electrochemical equilibra in aqueous solution, NACE Cebelcor. Houston, 1974, 10.

[2] K. Nisancioglu, Corrosion of aluminium alloys, *Proceedings of ICAA* 3, 3 **(**1992) 239-259

[3] G. K. Gomma, *Materials Chemistry and Physics* 55 **(**1998) 241-246

[4] S. A. Umoren, O. Ogbobe, E. E. Ebenso and U. J. Ekpe, *Pigment and Resin Technology* 35 (2006) 284-292

[5] M. A. Chidiebere, E. E. Oguzie, L. Liu, Y. Li, F. Wang, *Industrial and Engineering Chemistry Research* 51 (2014) 668-677

[6] E. E. Ebenso, *Nigerian Journal of Chemical Research* 6 (2001) 8-12

[7] E. E. Oguzie, G. N. Onuoha, A.I, Onuchukwu, *Materials Chemistry and Physics* 89 (2005) 305-311.

[8] E. E. Oguzie, D. I. Njoku, M. A. Chidiebere, C. E. Ogukwe, G. N. Onuoha, K. L. Oguzie, N. Ibisi, *Industrial and Engineering Chemistry Research* 53 (2014) 5886-5894

[9] S. A. Umoren, Y. Li, F. H. Wang, *Journal of Solid State Electrochemistry* 14 (2010) 2293-2305

[10] E. E. Oguzie, S. G. Wang, Y. Li, F. H. Wang, *Journal of Physical Chemistry C*. 113 (2009) 8420 -8429

[11] L. M. D André; R. M. Jivaldo, *Brazilian Journal of Pharmaceutical Sciences* 49 (2013) 275-283

[12] M. Hongyun, Y. Shouzhi, Z. Qin, *Advanced Materials Research* 194 (2011) 134-138

[13] H. Sheng; X. Kang; C. Fu, *Journal of Chinese Society of Corrosion and Protection*, 29 (2009) 149-153

[14] K. F. Khaled, *Electrochimica Acta.* 55 (2010) 6523-6532

[15] E. E. Oguzie, C. K. Enenebeaku, C. O.Akalezi, S. C.Okoro, A. A. Ayuk; E. N. Ejike, *Journal of Colloid Interface Science* 349 (2010) 283-292

[16] S. A. Umoren; E. E. Ebenso, *Materials Chemistry and Physics*, 106 (2007) 387-393

[17] R. Solmaz, M. E. Mert, G. Kardas, B. Yazici, M. Brbil, *Acta Physico-Chimica Sinica* 24 (2008) 1185-1191

[18] M. C. Chidiebere, E. C. Ogukwe; K. L.Oguzie, N. E Chukwuemeka, E. E Oguzie, *Industrial and Engineering Chemistry Research* 51 (2012) 668-677

[19] A. Saviour Umoren, M. G. Zuhair, I. B. Obot, *Industrial and Engineering Chemistry Research* 52 (2013) 14855-14865

[20] N. A. Negam, N. G. Kandile, I. A. Aiad, M. A. Mohammad, *Colloids and Surfaces* A391 (2011) 224-233

[21] H. K. Sappani, K. Sambantham, *Industrial and Engineering Chemistry Research* 52 (2013) 7457-7469

[22] I. B. Obot, N.O. Obi-Egbedi, *Corrosion Science* 52 (2010) 198-204

[23] Z. Tao, S. Zhang, W. Li, B. Hou, *Industrial and Engineering Chemistry Research* 50 (2011) 6082-6088

[24] M. Kissi, M. Bouklah, B. Hammouti, M. Benkaddour, *Applied Surface Science* 252 (2006) 4190-4197

[25] R. A. Prabhu, T. V. Venkatesha, A. V. Shanbhag, B. M. Praveen, G. M. Kulkarni, R. G. Kalkhambkar. *Materials Chemistry and Physics* 108 (2008) 283-289

[26] G. Moretti, F. Guidi, G. Grion, *Corrosion Science* 46 (2003) 387-403

[27] R. Jasinski, A. Lob, *Journal Electrochemical Society* 135 (1988) 551-556

[28] A. Asan, M. Kabasakalog ˘lu, M. Isıklan, Z. Kılıç, *Corrosion Science* 2005, 47, 1534-1544

[29] G. Kardas, R. Solmaz, *Corrosion Revision* 24 (2006) 151-171

[30] R. Solmaz, G. Kardas, M. Culha, B. Yazici, M. Erbil, *Electrochimica Acta* 53 (2008) 5941-5952

[31] N. A. Negm, Y. M. Elkholy, M. K. Zahran, S. M. Tawfik, *Corrosion Science* 52 (2010) 3523-3536

[32] N. O. Obi-Egbedi, I. B. Obot, *Corrosion Science* 53 (2011) 263-275

[33] M. Özcan, F. Karadag, I. Dehri, *Acta Physico Chimica Sinica* 24 (2008) 1387-1393

[34] X. Wang, H. Yang, F. Wang, *Corrosion Science* 53 (2011) 113-121

[35] M. Özcan, R. Solmaz, G. Kardas, I. Dehri, *Colloids Surfaces* 325 (2008) 57-63

[36] S. Deng, X. Li, H. Fu, *Corrosion Science* 53 (2011) 822-828

(Received 30 September 2017; accepted 16 October 2017)